

Production of two charm quark-antiquark pairs in single-parton scattering within the k_t -factorization approach

Andreas van Hameren,^{1,*} Rafał Maciuła,^{1,†} and Antoni Szczurek^{2,‡}

¹*Institute of Nuclear Physics PAN, PL-31-342 Cracow, Poland*

²*Institute of Nuclear Physics PAN, PL-31-342 Cracow, Poland and
University of Rzeszów, PL-35-959 Rzeszów, Poland*

(Dated: April 29, 2015)

Abstract

We present first results for the $2 \rightarrow 4$ single-parton scattering $gg \rightarrow c\bar{c}c\bar{c}$ subprocess for the first time fully within the k_t -factorization approach. In this calculation we have used the Kimber-Martin-Ryskin unintegrated gluon distribution which effectively includes some class of higher-order gluon emissions, and an off-shell matrix element squared calculated using recently developed techniques. The results are compared with our earlier result obtained within the collinear-factorization approach. Only slightly larger cross sections are obtained than in the case of the collinear approach. Inclusion of transverse momenta of gluons entering the hard process leads to a much stronger azimuthal decorrelation between cc and $\bar{c}\bar{c}$ than in the collinear-factorization approach. A comparison to predictions of double parton scattering (DPS) results and the LHCb data strongly suggests that the assumption of two fully independent DPS ($gg \rightarrow c\bar{c} \otimes gg \rightarrow c\bar{c}$) may be too approximate.

PACS numbers: 13.87.Ce, 14.65.Dw

*Electronic address: andreas.hameren@ifj.edu.pl

†Electronic address: rafal.maciula@ifj.edu.pl

‡Electronic address: antoni.szczurek@ifj.edu.pl

I. INTRODUCTION

At high energy, gluon-gluon fusion becomes the dominant mechanism of heavy $c\bar{c}$ or $b\bar{b}$ pair production. The cross section for single pair production can be calculated either in collinear next-to-leading order approach or the k_t -factorization approach. The $Q\bar{Q}$ and Higgs production are golden reactions for applications of the k_t -factorization approach [1–14]. In the k_t -factorization approach the basic ingredients are so-called unintegrated gluon distribution functions (UGDFs) and off-shell matrix elements. Different models of UGDFs have been proposed in the literature. The Kimber-Martin-Ryskin (KMR) [15] UGDF is believed to include the dominant higher-order corrections. The off-shell matrix elements for $gg \rightarrow Q\bar{Q}$ were calculated already long ago [1–3]. The k_t -factorization formalism was applied recently in the context of experimental data measured at the LHC [16–20] and a relatively good description was obtained when using the KMR UGDF.

In the case of the Higgs boson production both $2 \rightarrow 1$ and $2 \rightarrow 2$ subprocess have to be taken into account [14]. In Ref. [21] a $2 \rightarrow 3$ $gg \rightarrow c\bar{c}\gamma$ subprocess was taken into account when calculating cross sections for $pp \rightarrow c\bar{c}\gamma X$ reaction. Recently the k_t -factorization approach was also applied to three-jet [22] and $Zb\bar{b}$ [23] production.

A convenient formalism for the automation of the calculation of tree-level scattering amplitudes with off-shell gluons for arbitrary processes was recently introduced in Ref. [24]. Off-shell gluons are replaced by eikonal quark-antiquark pairs, and the amplitude can be calculated with the help of standard local Feynman rules, including the eikonal gluon-quark-antiquark vertex and the eikonal quark-antiquark propagator. The well-known successful recursive methods to calculate tree-level amplitudes can directly be applied, including the “on-shell” recursion, or Britto-Cachazo-Feng-Witten recursion, as shown in Ref. [25]. The heuristic introduction of the formalism in Ref. [24] has been given solid ground in Ref. [26]. Most of the effort was devoted to dijet production [27, 28] so far.

The $pp \rightarrow c\bar{c}c\bar{c}X$ reaction is interesting by itself. It was shown by us recently that this reaction is a golden reaction to study double-parton scattering (DPS) processes [29, 30]. The LHCb collaboration confirmed the theoretical predictions and obtained a large cross section for production of two mesons, both containing c quarks or both containing \bar{c} antiquarks [31]. The single-parton scattering (SPS) contribution was discussed in Refs. [32]

and [33]. In the first case [32] a high-energy approximation was used neglecting some unimportant at high energies Feynman diagrams. Last year we have calculated the lowest-order SPS cross section(s) including a complete set of Feynman diagrams [33] in the collinear-factorization approach. The final result was only slightly different than that obtained in the high-energy approximation.

In the present letter we wish to go one step further and try to calculate the SPS cross sections for the $pp \rightarrow c\bar{c}c\bar{c}X$ reaction consistently in the k_t -factorization approach. Doing so we may hope that a sizeable part of higher-order corrections will be included. On the technical side this will be a first calculation within the k_t -factorization approach based on a $2 \rightarrow 4$ subprocesses with two off-shell initial-state partons (gluons). The result is also important in the context of studying DPS as the considered SPS mechanism constitutes an irreducible background, and its estimation is therefore of prior importance if deeper conclusions concerning DPS can be drawn from measurements at the LHC.

II. FORMALISM

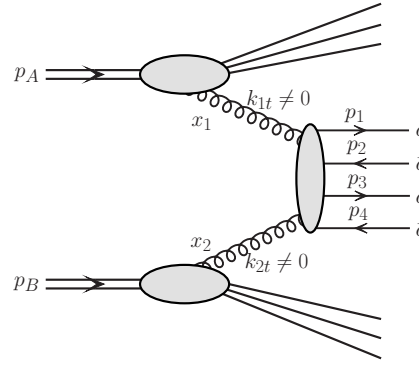


FIG. 1: A diagrammatic representation of the considered mechanism of $c\bar{c}c\bar{c}$ final-state production via single-parton scattering within k_t -factorization approach.

Within the k_t -factorization approach the SPS cross section for $pp \rightarrow c\bar{c}c\bar{c}X$ reaction, sketched in Fig. 1, can be written as

$$d\sigma_{pp \rightarrow c\bar{c}c\bar{c}} = \int dx_1 \frac{d^2 k_{1t}}{\pi} dx_2 \frac{d^2 k_{2t}}{\pi} \mathcal{F}(x_1, k_{1t}^2, \mu^2) \mathcal{F}(x_2, k_{2t}^2, \mu^2) d\hat{\sigma}_{g g \rightarrow c\bar{c}c\bar{c}}. \quad (2.1)$$

In the formula above $\mathcal{F}(x, k_t^2, \mu^2)$ are unintegrated gluon distributions that depend on longitudinal momentum fraction x , transverse momentum squared k_t^2 of the gluons entering the hard process, and in general also on a (factorization) scale of the hard process

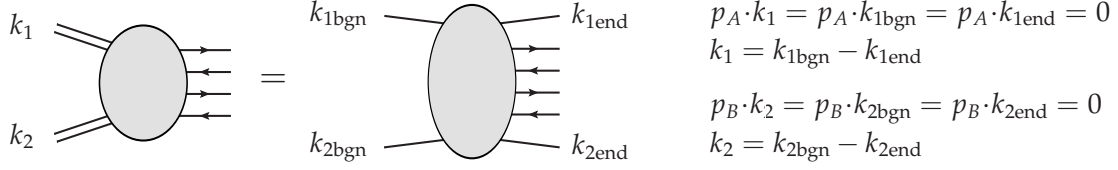


FIG. 2: Momenta of the off-shell gluons, represented as double lines on the left hand side, and the eikonal quark-antiquark pairs. The amplitude is independent of a simultaneous momentum shift $k_{1\text{bgn}} + q, k_{1\text{end}} + q$ as long as $p_A \cdot q = 0$. The same holds for the other eikonal line with p_B .

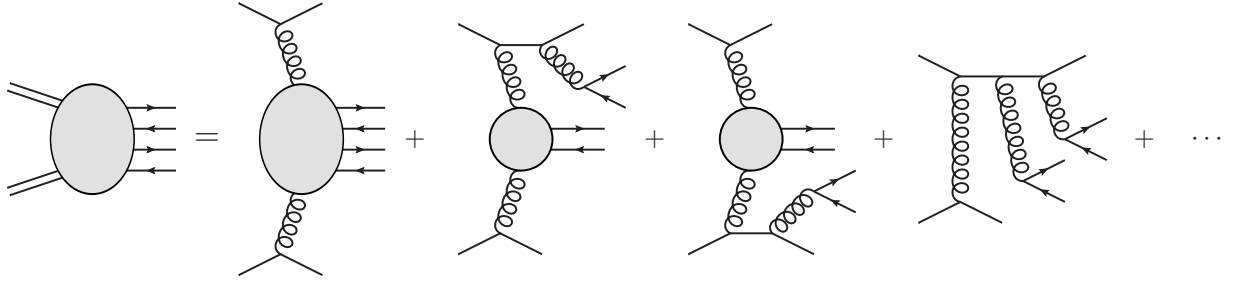


FIG. 3: Some terms in the expansion of the amplitude in terms of the eikonal propagators. The eikonal quarks are denoted by lines without arrows. The double lines on the left hand side represent the off-shell gluons. This expansion does not represent the organization of the calculation, and only gives an impression of which graphs are included.

μ^2 . The elementary cross section in Eq. (2.1) can be written somewhat formally as:

$$d\hat{\sigma} = \frac{d^3 p_1}{2E_1(2\pi)^3} \frac{d^3 p_2}{2E_2(2\pi)^3} \frac{d^3 p_3}{2E_3(2\pi)^3} \frac{d^3 p_4}{2E_4(2\pi)^3} (2\pi)^4 \delta^4(p_1 + p_2 + p_3 + p_4 - k_1 - k_2) \times \frac{1}{\text{flux}} |\overline{\mathcal{M}}_{g^* g^* \rightarrow c\bar{c}c\bar{c}}(k_1, k_2)|^2, \quad (2.2)$$

where only dependence of the matrix element on four-vectors of gluons k_1 and k_2 is made explicit. In general all four-momenta associated with partonic legs enter. The matrix element takes into account that both gluons entering the hard process are off-shell with virtualities $k_1^2 = -k_{1t}^2$ and $k_2^2 = -k_{2t}^2$. The matrix element squared is rather complicated and explicit formula will be not given here.

As mentioned in the introduction, the scattering amplitudes with off-shell initial state gluons are constructed using the formalism of Ref. [24], in which off-shell gluons are represented by eikonal quark-antiquark pairs in order to arrive at gauge invariant ampli-

tudes. Figure 3 gives an idea of what kind of graphs are included. The Feynman rules related to the eikonal quark-antiquark-gluon vertex and eikonal propagator are

$$\begin{array}{c} i \\ \diagdown \\ \text{-----} \mu, b \\ \diagup \\ j \end{array} = -ip_A^\mu T_{i,j}^b \quad , \quad \xrightarrow{K} = \frac{i}{p_A \cdot K} \quad , \quad (2.3)$$

where p_A is the longitudinal momentum associated with the off-shell gluon. The external eikonal quark-antiquark pairs carry fundamental color indices, say i, j . It was noted in Ref. [34] that the amplitude is traceless with respect to these indices, so an adjoint color index can be assigned to the off-shell gluon by contracting the amplitude with $\sqrt{2}T_{ij}^a$. The squared amplitude summed over colors gives the same result. Denoting by \mathcal{M}^a the amplitude with the color of one off-shell gluon highlighted explicitly we have

$$\sum_a |\mathcal{M}^a|^2 = \sum_a \left| \sqrt{2} \sum_{i,j} \mathcal{M}_{ij} T_{ij}^a \right|^2 = \sum_{i,j,k,l} \mathcal{M}_{ij} \mathcal{M}_{kl}^* \left(\delta_{ik} \delta_{lj} - \frac{1}{N_c} \delta_{ij} \delta_{kl} \right) = \sum_{i,j} |\mathcal{M}_{ij}|^2. \quad (2.4)$$

The first term on the right hand side of Fig. 3 contains the “actual off-shell gluons” as virtual gluons, representing complete propagators. This term would diverge if $k_{1t}^2 \rightarrow 0$ and/or $k_{2t}^2 \rightarrow 0$, so the whole amplitude has to be multiplied with $\sqrt{k_{1t}^2 k_{2t}^2}$ to reproduce correct collinear limit.

The calculation has been performed with the help of A Very Handy LIBrary [34]. In this Fortran library, scattering amplitudes are calculated numerically as a function of the external four-momenta via Dyson-Schwinger recursion [35]. It is a recursion of off-shell currents, which automatically factorizes the calculation of the sum of all Feynman graphs such that the multiplications represented by vertices are executed only once for each vertex, while such vertex may occur in several graphs, for identical kinematics. This recursion is sketched in Fig. 4 and Fig. 5. The auxiliary eikonal quarks and anti-quarks are treated as external particles, so eventually an eight-point amplitudes are calculated. AVHLIB allows for various choices of the representation of the external helicities and colors. These include both the color-ordered representation [36, 37], with exact summation over color, and the color-dressed representation [38, 39], with Monte Carlo summation for large multiplicities. Helicity configurations can be summed exactly, or, again for large multiplicities, treated in a Monte Carlo approach, both discrete and with continuous random polarizations [40]. The library includes a full Monte Carlo program with an adaptive

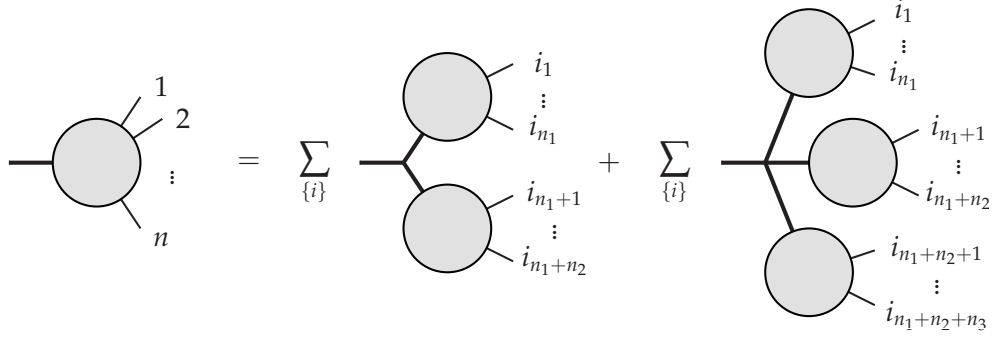


FIG. 4: Dyson-Schwinger recursion for off-shell currents. The thick lines represent off-shell (virtual) particles and the thin lines represent on-shell external particles. The sum is over all partitions of these external particles over the different blobs and all flavors for the virtual particles that are allowed according to the Feynman rules.

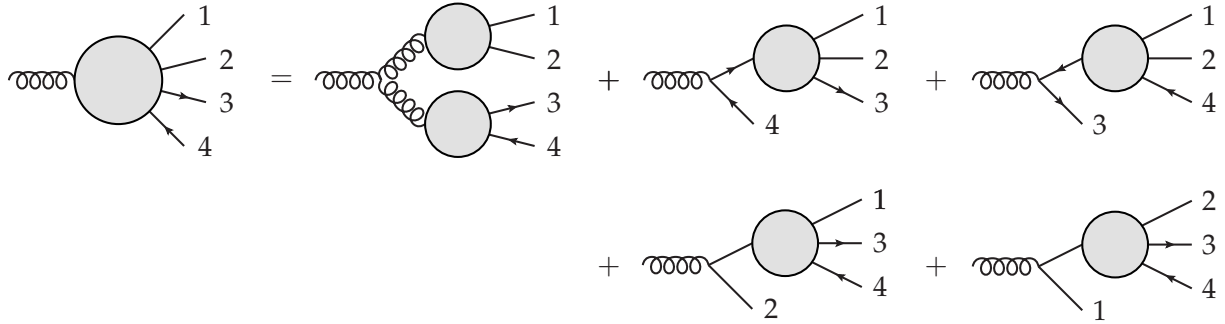


FIG. 5: An explicit example of one Dyson-Schwinger recursive step for a certain off-shell current.

phase space generator [41, 42] that deals with the integration variables related to both the initial-state momenta and the final-state momenta.

The program can also conveniently generate a file of unweighted events, which approach was used for the analysis presented in this paper. In the present calculation we use: $\mu_f^2 = (\sum_i^4 m_{i,t})^2$ as the factorization scale and $m_c = 1.5$ GeV in both k_t -factorization and in the reference collinear-factorization calculations. Uncertainties related to the choice of the parameters were discussed e.g. in Ref. [33] and will be not considered here. Here we wish to concentrate on the relative effect and modifications with respect to the results of the collinear-factorization calculations presented already in the literature [32, 33].

III. FIRST RESULTS

In this section we wish to compare the new results of the k_t -factorization approach to those obtained by us in Ref. [33] in the collinear-factorization approach.

In Fig. 6 we show standard single particle distributions in charm quark/antiquark transverse momentum (left panel) and its rapidity (right panel). We predict an enhancement of the cross section at large transverse momenta of c or \bar{c} compared to the collinear-factorization approach. The rapidity distributions in both approaches are rather similar (see the left panel of the figure).

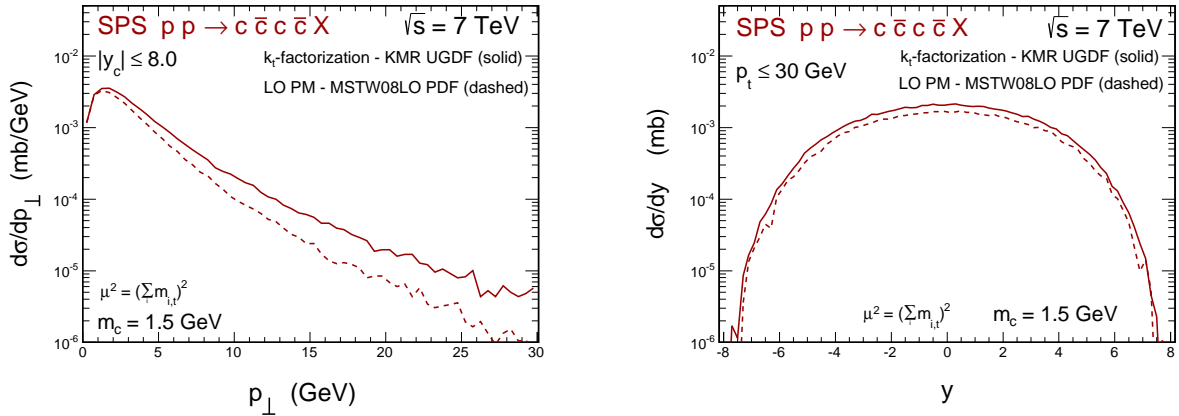


FIG. 6: Distributions in c quark (\bar{c} antiquark) transverse momentum (left panel) and rapidity (right panel). The k_t -factorization result (solid line) is compared with the collinear-factorization result (dashed line).

Distributions in rapidity of the cc (or $\bar{c}\bar{c}$) and $c\bar{c}$, defined as $Y_{cc} = (y_c + y_{\bar{c}})/2$ and $Y_{c\bar{c}} = (y_c + y_{\bar{c}})/2$ respectively, are shown in Fig. 7. The distributions are much narrower than those for single quark/antiquark which reflects the fact that the two different c quarks (or two different \bar{c} antiquarks) have typically different rapidities. The discussed distributions in y_c and Y_{cc} would be identical only if $y_{c,1} = y_{c,2}$ (strong rapidity correlations). This will become clearer when inspecting rapidity difference in the next plots.

Similar distributions but for rapidity distance between two c quarks (or two \bar{c} antiquarks) and between c and \bar{c} are shown in Fig. 8. On average the distance between c and c is larger than that for c and \bar{c} . This can be understood easily in the high-energy approximation discussed in Ref. [32] by inspecting the contributing diagrams. Some enhancement at small rapidity separations can be observed in the k_t -factorization approach

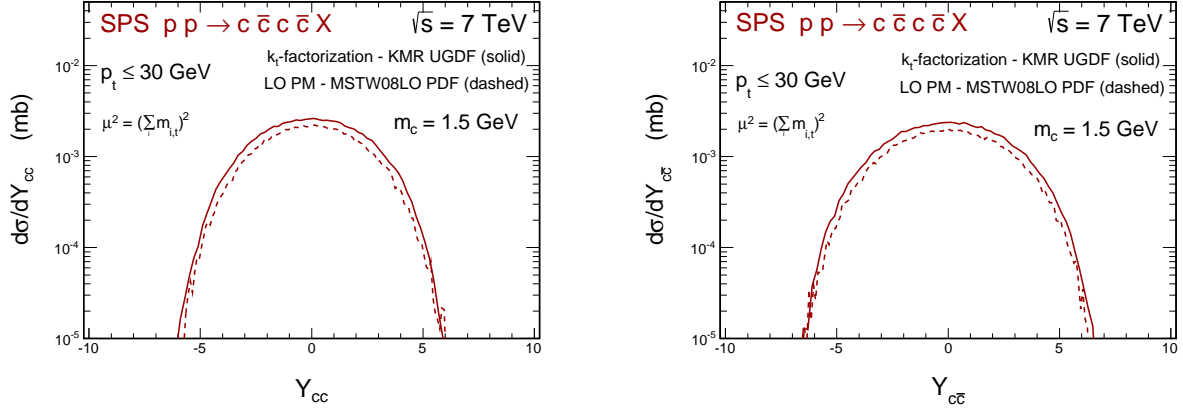


FIG. 7: Distributions in rapidity $Y_{cc} = (y_c + y_c)/2$ (left panel) and $Y_{c\bar{c}} = (y_c + y_{\bar{c}})/2$ (right panel). The meaning of the curves is the same as in Fig. 6.

compared to the collinear approach.

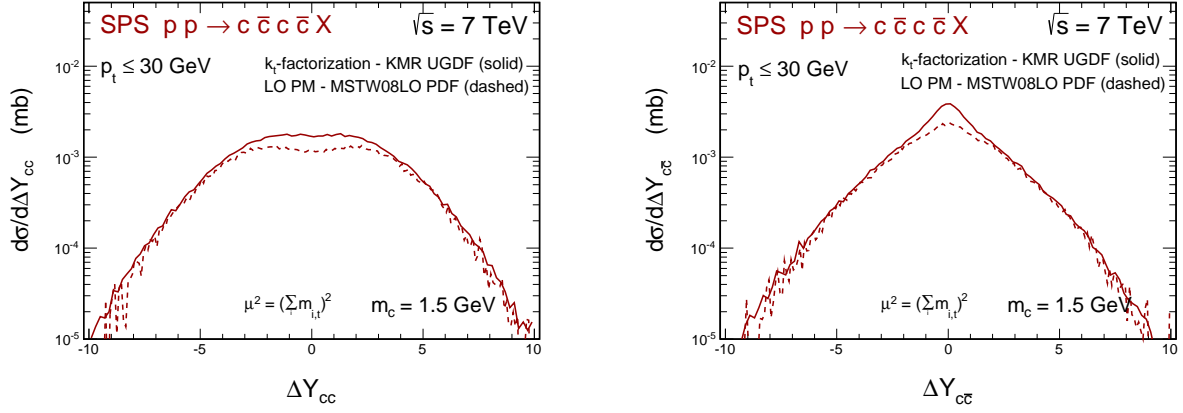


FIG. 8: Distributions in the difference of rapidities $\Delta Y_{cc} = y_c - y_c$ (left panel) and $\Delta Y_{c\bar{c}} = y_c - y_{\bar{c}}$ (right panel). The meaning of the curves is the same as in Fig. 6.

The distributions in rapidity distance are strongly correlated with M_{cc} or $M_{c\bar{c}}$ distributions shown in Fig. 9. Those distribution are, however, difficult to measure as rather mesons are measured and not quarks or antiquarks.

Quite interesting are azimuthal angle correlations between c and c or c and \bar{c} . The corresponding distributions are shown in Fig. 10. We note much bigger decorrelation of two c quarks or c and \bar{c} in the k_t -factorization approach compared to the collinear approach. This is due to explicit account of gluon virtualities (transverse momenta). We will return to this point when discussing azimuthal correlations between mesons at the

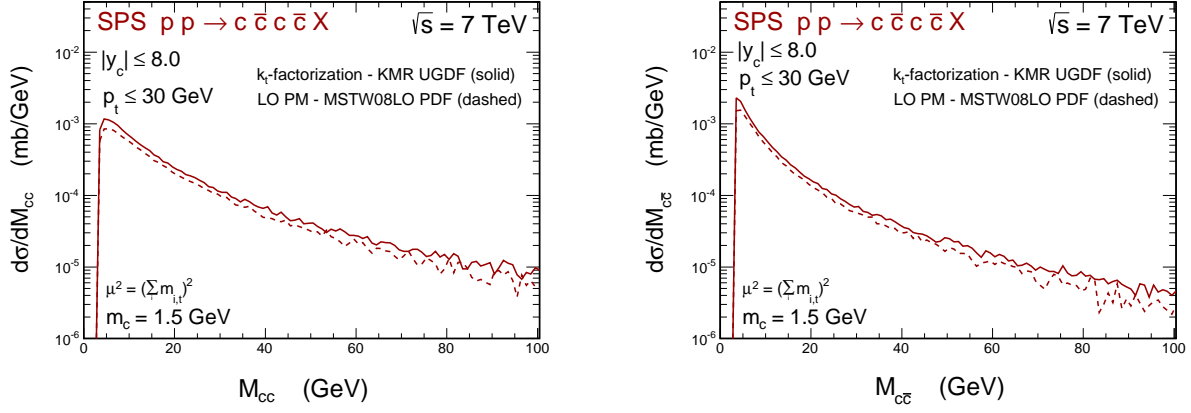


FIG. 9: Invariant mass distributions in M_{cc} (left panel) and $M_{c\bar{c}}$ (right panel). The meaning of the curves is the same as in Fig. 6.

end of this section.

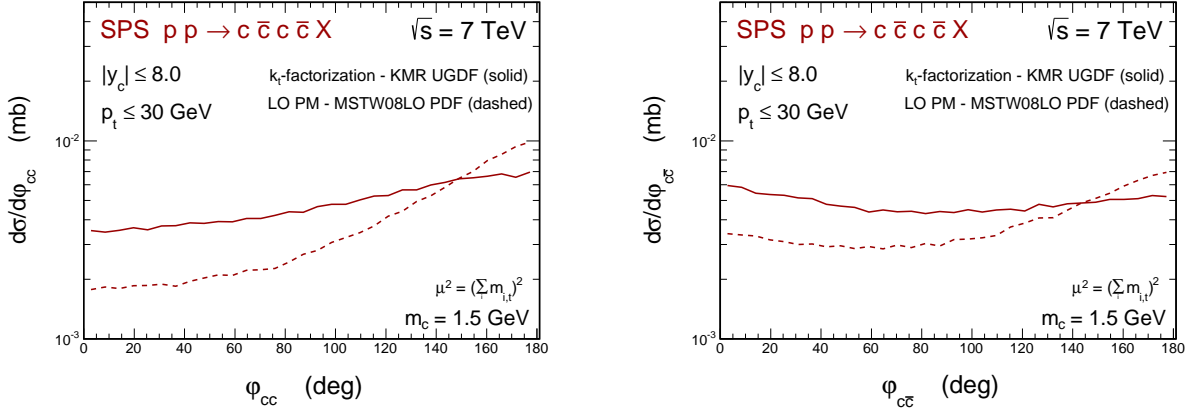


FIG. 10: Azimuthal angle correlations between two c quarks (left panel) and between c and \bar{c} (right panel). The meaning of the curves is the same as in Fig. 6.

Next we wish to visualize the regions of the transverse momenta of initial gluons that give sizeable contribution to the SPS $pp \rightarrow c\bar{c}c\bar{c}X$ cross section. In Fig. 11 we show a two-dimensional distribution in initial-gluon transverse momenta. The dependence on k_{1t} and k_{2t} shown in the figure is determined by the UGDF used in the calculation as well as by the dependence of the matrix element on k_{1t} and k_{2t} . Other models of unintegrated gluon distributions would give different dependencies. Clearly we get large contributions from the regions far from the collinear case ($k_{1t} = 0$ and $k_{2t} = 0$). This has of course consequences for other observables discussed above through the dependence of the matrix element on

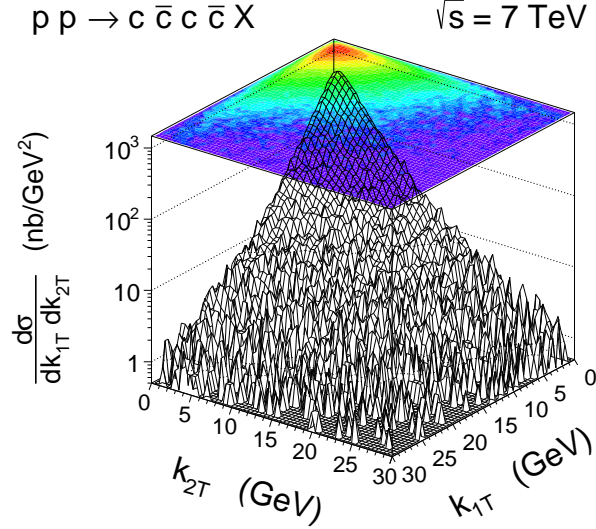


FIG. 11: Two-dimensional distribution in transverse momenta of initial gluons in the $pp \rightarrow c\bar{c}c\bar{c}X$ SPS process at $\sqrt{s} = 7$ TeV.

the gluon transverse momenta $|\overline{\mathcal{M}(k_{1t}, k_{2t})}|^2$ and its correlation with other kinematical variables.

We will not discuss in the present letter the correlations between the gluon virtualities (or their transverse momenta) and other kinematical variables related to the charm quarks and antiquarks.

So far we have considered production of $c\bar{c}c\bar{c}$ quarks/antiquarks. As discussed in our previous paper [33] such a final states may lead to the production of two D mesons, both containing c quarks or both containing \bar{c} antiquarks which is not possible e.g. for the $c\bar{c}$ final-state case. As explained in Ref. [33] the DPS gives cross sections very similar to those measured by the LHCb collaboration [31]. How important is the SPS contribution discussed in this paper, calculated here in the k_t -factorization, is shown in Fig. 12. For comparison we show also SPS results calculated in collinear-factorization approach [33]. The two approaches give somewhat different shapes of correlation observables, inspite that the integrated cross sections are rather similar as discussed already at the parton level. Our results, so far the most advanced in the literature as far as the SPS contribution is considered, are not able to explain discrepancy between DPS contribution and the LHCb experimental data. If the discrepancies are due to simplifications in the treat-

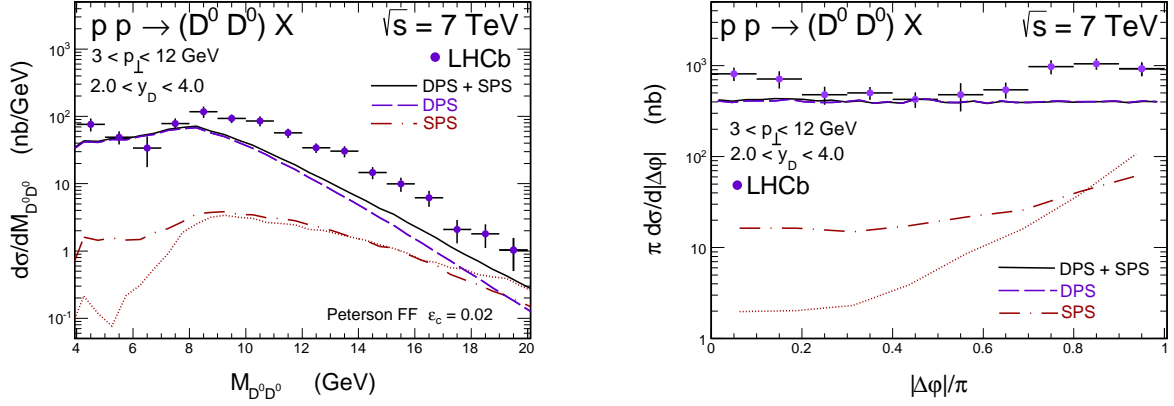


FIG. 12: Distributions in $D^0 D^0$ invariant mass (left) and in azimuthal angle between both D^0 's (right) within the LHCb acceptance. The DPS contribution (dashed line) is compared with the SPS one calculated within the k_t -factorization approach (dashed-dotted line). The SPS result from our previous studies [33], calculated in the LO collinear-factorization approach, is also shown here (dotted line).

ment of DPS requires further studies including for example spin and flavour correlations. Some works in this direction already started [43].

IV. CONCLUSIONS

In the present paper we have made a first calculation of the cross section for $pp \rightarrow c\bar{c}c\bar{c}X$ in the k_t -factorization approach, i.e. focussing on single parton scattering process. This is a first $2 \rightarrow 4$ process for which k_t -factorization is applied. In this calculation we have used the Kimber-Martin-Ryskin unintegrated gluon distribution(s) which effectively takes into account the dominant higher-order corrections. The off-shell matrix element was calculated using a new technique developed recently in Kraków.

The results of the k_t -factorization approach were compared with the results of the collinear-factorization approach. In general, the k_t -factorization results are only slightly bigger than those for collinear approach. An exception is the transverse momentum distribution above 10 GeV where a sizeable enhancement has been observed. Inclusion of gluon virtualities leads to a decorrelation in azimuthal angle between c and c or c and \bar{c} .

Since the cross section is in general very similar as for the collinear-factorization approach we conclude that the $c\bar{c}c\bar{c}$ final state at the LHC energies is dominantly produced

by the double parton scattering as discussed in our recent papers, and the SPS contribution, although interesting by itself, is rather small. A comparison to predictions of double-parton scattering results and recent LHCb data for azimuthal angle correlations between D^0 and D^0 or \bar{D}^0 and \bar{D}^0 mesons strongly suggests that the assumption of two fully independent DPS ($gg \rightarrow c\bar{c} \otimes gg \rightarrow c\bar{c}$) may be too approximate or even not valid. Some possible reasons were discussed in Ref. [43]. The effect found there is, however, too small to explain a rather large effect observed by the LHCb collaboration. This remains a challenge for future theoretical studies and should be confirmed by the LHCb collaboration at $\sqrt{s} = 13, 14$ TeV.

Acknowledgments

This study was partially supported by the Centre for Innovation and Transfer of Natural Sciences and Engineering Knowledge in Rzeszów. Graphs were drawn with the help of Jaxodraw.

-
- [1] S. Catani, M. Ciafaloni and F. Hautmann, Nucl. Phys. **366**, 135 (1991).
 - [2] J.C. Collins and R.K. Ellis, Nucl. Phys. **B360**, 3 (1991).
 - [3] R.D. Ball and R.K. Ellis, J. High Energy Phys. **05**, 053 (2001).
 - [4] Ph. Hägler, R. Kirschner, A. Schäfer, I. Szymanowski and O.V Teryaev, Phys. Rev. **D62**, 071502 (2000).
 - [5] S.P. Baranov and M. Smizanska, Phys. Rev. **D62**, 014012 (2000).
 - [6] N. P. Zotov, A. V. Lipatov and V. A. Saleev, Phys. Atom. Nucl. **66**, 755 (2003) [Yad. Fiz. **66**, 786 (2003)].
 - [7] S.P. Baranov, A.V. Lipatov and N.P. Zotov, Phys. Atom. Nucl. **67**, 837 (2004) [Yad. Fiz. **67**, 856 (2004)].
 - [8] M. Łuszczak and A. Szczurek, Phys. Rev. **D73**, 054028 (2006).
 - [9] Yu.M. Shabelski and A.G. Shuvaev, Phys. Atom. Nucl. **69**, 314 (2006).
 - [10] M. Łuszczak, R. Maciuła and A. Szczurek, Phys. Rev. **D79**, 034009 (2009).
 - [11] R. Maciuła, A. Szczurek and G. Ślipek, Phys. Rev. **D83**, 054014 (2011).
 - [12] R. S. Pasechnik, O. V. Teryaev and A. Szczurek, Eur. Phys. J. C **47**, 429 (2006).

- [13] A. V. Lipatov, M. A. Malyshev and N. P. Zotov, Phys. Lett. B **735**, 79 (2014).
- [14] A. Szczurek, M. Łuszczak and R. Maciuła, Phys. Rev. D **90**, 094023 (2014).
- [15] M.A. Kimber, A.D. Martin and M.G. Ryskin, Phys. Rev. **D63**, 114027 (2001).
- [16] H. Jung, M. Kraemer, A.V. Lipatov and N.P. Zotov, Phys. Rev. **D85**, 034035 (2012);
J. High Energy Phys. **01**, 085 (2011).
- [17] V. Saleev and A. Shipilova, Phys. Rev. D **86**, 034032 (2012).
- [18] R. Maciuła, and A. Szczurek, Phys. Rev. **D87**, 094022 (2013).
- [19] A. V. Karpishkov, M. A. Nefedov, V. A. Saleev and A. V. Shipilova, Phys. Rev. D **91**, 054009 (2015).
- [20] A. V. Karpishkov, M. A. Nefedov, V. A. Saleev and A. V. Shipilova, Int. J. Mod. Phys. A **30**, 1550023 (2015).
- [21] S. P. Baranov, A. V. Lipatov and N. P. Zotov, Eur. Phys. J. C **56**, 371 (2008).
- [22] A. van Hameren, P. Kotko and K. Kutak, Phys. Rev. D **88**, 094001 (2013) [Phys. Rev. D **90**, 039901 (2014)].
- [23] A. V. Lipatov and N. P. Zotov, arXiv:1501.05130 [hep-ph].
- [24] A. van Hameren, P. Kotko and K. Kutak, J. High Energy Phys. **01**, 078 (2013) [arXiv:1211.0961 [hep-ph]].
- [25] A. van Hameren, J. High Energy Phys. **07**, 138 (2014) [arXiv:1404.7818 [hep-ph]].
- [26] P. Kotko, J. High Energy Phys. **07**, 128 (2014) [arXiv:1403.4824 [hep-ph]].
- [27] A. van Hameren, P. Kotko, K. Kutak, C. Marquet and S. Sapeta, Phys. Rev. D **89**, 094014 (2014).
- [28] A. van Hameren, P. Kotko, K. Kutak and S. Sapeta, Phys. Lett. B **737**, 335 (2014).
- [29] M. Łuszczak, R. Maciuła, and A. Szczurek, Phys. Rev. **D85**, 094034 (2012).
- [30] R. Maciuła, and A. Szczurek, Phys. Rev. **D87**, 074039 (2013).
- [31] R. Aaij *et al.* (LHCb Collaboration), J. High Energy Phys. **06**, 141 (2012).
- [32] W. Schäfer, and A. Szczurek, Phys. Rev. **D85**, 094029 (2012).
- [33] A. van Hameren, R. Maciuła and A. Szczurek, Phys. Rev. D **89**, 094019 (2014).
- [34] M. Bury and A. van Hameren, arXiv:1503.08612 [hep-ph].
- [35] F. Caravaglios and M. Moretti, Phys. Lett. B **358** (1995) 332 [hep-ph/9507237].
- [36] A. Kanaki and C. G. Papadopoulos, AIP Conf. Proc. **583** (2001) 169 [hep-ph/0012004].
- [37] F. Maltoni, K. Paul, T. Stelzer and S. Willenbrock, Phys. Rev. D **67** (2003) 014026

- [hep-ph/0209271].
- [38] C. G. Papadopoulos and M. Worek, Eur. Phys. J. C **50** (2007) 843 [hep-ph/0512150].
- [39] C. Duhr, S. Hoeche and F. Maltoni, JHEP **0608** (2006) 062 [hep-ph/0607057].
- [40] P. Draggiotis, R. H. P. Kleiss and C. G. Papadopoulos, Phys. Lett. B **439** (1998) 157 [hep-ph/9807207].
- [41] A. van Hameren, Acta Phys. Polon. B **40** (2009) 259 [arXiv:0710.2448 [hep-ph]].
- [42] A. van Hameren, arXiv:1003.4953 [hep-ph].
- [43] M G. Echevarria, T. Kasemets, P. J. Mulders and C. Pisano, J. High Energy Phys. **04**, 034 (2015).